Taylor & Francis
Taylor & Francis Group

Vehicle System Dynamics
International Journal of Vehicle Mechanics and Mobility

ISSN: 0042-3114 (Print) 1744-5159 (Online) Journal homepage: https://www.tandfonline.com/loi/nvsd20

Coupled vibration analysis of Maglev vehicle-guideway while standing still or moving at low speeds

Ki-Jung Kim, Jong-Boo Han, Hyung-Suk Han & Seok-Jo Yang

To cite this article: Ki-Jung Kim, Jong-Boo Han, Hyung-Suk Han & Seok-Jo Yang (2015) Coupled vibration analysis of Maglev vehicle-guideway while standing still or moving at low speeds, Vehicle System Dynamics, 53:4, 587-601, DOI: 10.1080/00423114.2015.1013039

To link to this article: https://doi.org/10.1080/00423114.2015.1013039

Vehicle System Dynamics, 2015
Vol. 53, No. 4, 587–601, http://dx.doi.org/10.1080/00423114.2015.1013039

Taylor & Francis
Taylor & Francis Group

Coupled vibration analysis of Maglev vehicle-guideway while standing still or moving at low speeds

Ki-Jung Kim[a], Jong-Boo Han[a], Hyung-Suk Han[b*] and Seok-Jo Yang[a]

[a]*Department of Mechatronics Engineering, Chungnam National University, Daejeon, Republic of Korea;* [b]*Department of Magnetic Levitation and Linear Drive, KIMM, Daejeon, Republic of Korea*

(*Received 20 March 2014; accepted 25 January 2015*)

Dynamic instability, that is, resonance, may occur on an electromagnetic suspension-type Maglev that runs over the elevated guideway, particularly at very low speeds, due to the flexibility of the guideway. An analysis of the dynamic interaction between the vehicle and guideway is required at the design stage to investigate such instability, setting slender guideway in design direction for reducing construction costs. In addition, it is essential to design an effective control algorithm to solve the problem of instability. In this article, a more detailed model for the dynamic interaction of vehicle/guideway is proposed. The proposed model incorporates a 3D full vehicle model based on virtual prototyping, flexible guideway by a modal superposition method and levitation electromagnets including feedback controller into an integrated model. By applying the proposed model to an urban Maglev vehicle newly developed for commercial application, an analysis of the instability phenomenon and an investigation of air gap control performance are carried out through a simulation.

Keywords: EMS-type Maglev; flexible guideway; resonance; feedback control

1. Introduction

Many consider the contactless, eco-friendly Maglev vehicle to represent the future of rail transport. In general, a Maglev vehicle runs over an elevated guideway, as shown in Figure 1. Due to the structural characteristics of the guideway, the flexibility of the guideway significantly affects the ride quality and stability. In particular, in electromagnetic suspension (EMS) Maglev system, which is the magnetic forces vary inversely with the air gap, the vibration due to the deflection of the flexible guideway gives rise to a resonance while standing still or moving at low speeds.[1,2] This instability occurs when the natural frequency of one or more bogies and guideway get too close to each other, because the levitation gap is actively controlled independently by electromagnetics suspension with feedback controller for stable suspension.[3] In the previous study, this instability, which the levitation air gap became unstable as shown in Figure 2, was reported.[3] It is reported that this instability was also recorded in the CMS03A Maglev vehicle on the test line.[1] Recently, for the purpose of reducing initial capital cost and minimising environmental impact, the development of a slender guideway has become a significant goal before the commercial application of a Maglev

*Corresponding author. Email: hshan@kimm.re.kr

Figure 1. Maglev vehicle running over the elevated guideway.

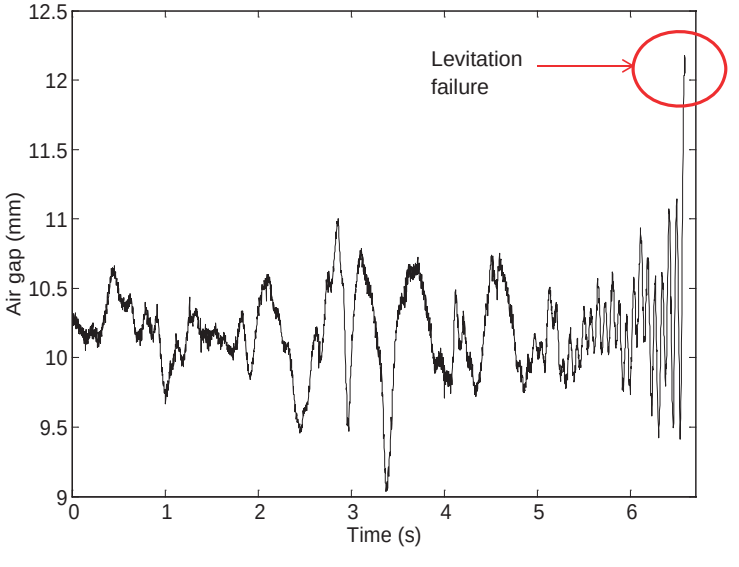

Figure 2. Air gap history of coupled resonance between Maglev and guideway.

vehicle. As the slender guideway particularly increases the flexibility and reduces mass, it has a strong effect on the running performance, and for this reason an in-depth investigation of running performance through a dynamic interaction analysis between the vehicle and guideway is required during the design process.

Over the past several decades, a considerable number of studies have been conducted on the dynamic interaction model of the vehicle-guideway, expanding in the direction from a simplified degree of freedom (DOF) model to multiple those. In the initial stage of research,

the vehicle model is simplified as a moving force or a moving mass.[4] In the simplified single electromagnet-beam coupled model, the electromagnetic force is simplified as a combination of a spring and a damper.[5,6] It can be said that the single electromagnet-beam models are helpful to analyse the principle underlying the dynamic interaction of vehicle-guideway. Since, more complex models have been established to represent the actual Maglev vehicle configuration. The electromagnet in these models is substituted with a sequence of the equivalent stiffness and damping in order to represent the distributed electromagnetic force.[7–10] The lateral movements of the vehicle are also considered in some studies.[11–13] These models are effective in investigating the lateral interaction of vehicle-guideway, and they are capable of evaluating the curve negotiation of a Maglev vehicle. Meanwhile, the elastic guideway is generally described as a single supported Bernoulli–Euler beam, because the length of the guideway is large compared to other dimensions, and the deflection of the guideway is very small compared to its length.[8,9] With the development of computer technology, vehicle-guideway interaction models based on the finite element (FE) and virtual prototyping method have been established.[13–17] These developed models have been found to be sufficiently precise to correspond with an actual vehicle. Although a considerable amount of research has already been performed on the dynamic interaction of vehicle-guideway, the instability problem of the Maglev system remains unsolved. Some researchers have reported that designing an effective control algorithm that can suppress the instability is useful to understand the underlying principle of the coupled vibration of Maglev and guideway.[1] For doing so, a detailed vehicle-guideway model with multi-DOF including the control may be required, and it is necessary to analyse the effects on the Maglev vehicle with a specific control system.

The purpose of this paper is to propose a more detailed model for analysing the dynamic interaction of vehicle-guideway, including the dynamic behaviour of a whole levitation system. The proposed dynamic model integrates a 3D full vehicle model, considering bodies, joints, and force elements based on prototyping, a flexible guideway by using a modal superposition and all levitation electromagnets including feedback controller, to represent the vehicle with a more realistic model. Applying the proposed model to an urban transit Maglev developed for a commercial application to analyse the instability of the vehicle, the similarity with the test results was confirmed and the air gap control performance of levitation system was investigated. Finally, the features of the model and some directions for future work were discussed.

2. Model

2.1. *Vehicle*

The vehicle model based on virtual prototyping is the most similar to the physical system, and includes all body, joint and nonlinear force elements. The bodies of the vehicle or bogie in particular can be represented as flexible, if necessary, to analyse the system vibration. The model also has the advantage of considering the structural vibration by the body deformation, i.e. the external force, inertia and internal force. The carbody is supported vertically on the sliding table, which in turn is mounted by air spring on top of both ends of the bogie frame, as shown in Figure 3. The bodies, mass and DOF are described in Table 1. The bogie consists of two side frames, four anti-roll beams, two linear induction motors, four air springs, two traction rods, and eight electromagnets. The left and right side frame are linked with each other using anti-roll beam. The spherical joints between side frames and anti-roll beams

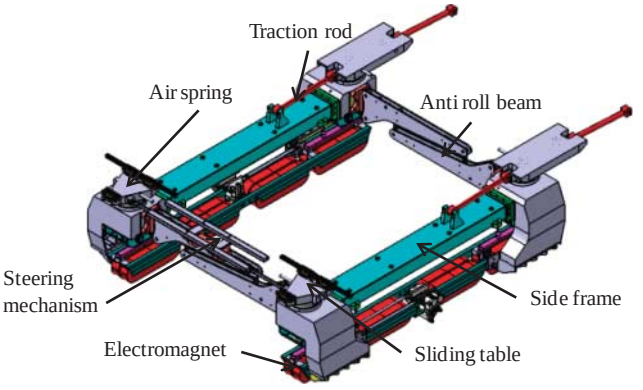

Figure 3. Multibody dynamic model for the bogie.

Table 1. Model data for the Maglev vehicle.

Item	Specification	Number	Element	Number
Cabin mass (kg)	11,000	2	Body	105
Bogie mass (kg)	2000	8	Bracket joints	25
Total of vehicles (kg)	38,000		Translational joints	20
			Spherical joints	64
Air spring stiffness (N/m)	Vertical: 62,000		Revolute joints	12
	Lateral: 140,000		Anti-roll beam bush	64
Air spring damping (kg/s)	Vertical: 1600		Air spring bush	32
	Lateral: 1300		Traction rod bush	32
			Total degree of freedom	128

are replaced with bushings to eliminate redundant constraints in the modelling. Other components such as secondary suspensions, joints, and bodies are modelled just like in conventional railway vehicles. The equations of motion for the vehicle have the form of the equations of constrained mechanical systems.[13,15] The Virtual Lab. Motion software is used in this study to employ automated formulation and solution of the system of equations of motion.

2.2. *Electromagnetic suspension*

Precise analysis of the suspension dynamics would require a nonlinear levitation force model, but a reasonably accurate linear model may be obtained by using linear approximations of the force for excursions around the nominal operating point (i_0, c_0).[13,18] Using these linear approximations, the changes in the levitation force and the current are expressed as Equations (1) and (2), respectively.

$$\begin{aligned} F_m(t) &= F_0 + \Delta F_m \\ &= \frac{\mu_0 A N^2}{4}\left(\frac{i_0}{c_0}\right)^2 + k_c \Delta c(t) - k_i \Delta i(t), \end{aligned} \tag{1}$$

where F_0 is the static force(N) at the nominal operating point, and ΔF_m is the controlled electromagnet force (N), i_0 is the nominal current(A) and c_0 is the nominal air gap(mm). μ_0 is the permeability factor, and A (m^2) is the section area of the magnetic pole, N is the number

of turns coil.

$$\Delta\dot{i}(t) = \frac{k_c}{k_i}\Delta\dot{c}(t) - \frac{R}{L_0}\Delta i(t) + \frac{1}{L_0}\Delta v(t), \tag{2}$$

where,

$$L_0 = \frac{\mu_0 N^2 A}{2c_0}, \quad k_i = \frac{\mu_0 N^2 A i_0}{2c_0^2}, \quad k_c = \frac{\mu_0 N^2 A {i_0}^2}{2c_0^3}.$$

The EMS system is inherently unstable, since the levitation force produced by a constant current and air gap are inversely related. Consequently the system is required feedback controller for stable suspension.[18] The levitation controller that employs the five-state feedback control law determines the voltage to control the current to maintain the air gap variation within an allowable deviation, as in Equation (3).

$$\Delta v(t) = k_1\Delta\hat{\ddot{q}}_m(t) + k_2\Delta\hat{\dot{q}}_m(t) + k_3\Delta\hat{q}_m(t) + k_4\Delta\hat{\dot{c}}(t) + k_5\Delta\hat{c}(t) \tag{3}$$

where $\Delta\hat{\ddot{q}}_m(t)$ is the observed acceleration, $\Delta\hat{\dot{q}}_m(t)$ the observed velocity, $\Delta\hat{q}_m(t)$ the observed position, $\Delta\hat{\dot{c}}(t)$ the observed air gap velocity, $\Delta\hat{c}(t)$ the observed air gap and k_1, k_2, k_3, k_4, k_5 the control gains.

To estimate reliably the five states variables, a dynamic filter is employed as in Equation (4) and (5). The five states to be used in the control law are estimated by the dynamic filter using the electromagnet vertical acceleration and the air gap, which are measured as input. The parameters in the filter are determined by cut-off frequency of gains for estimation the electromagnet vertical acceleration. That is, the acceleration of the electromagnet is estimated either by high-pass filter in high frequency domain or by replacing with the second derivative of air gap with low-pass filer in low frequency. Once the five states are estimated, the control law is designed in consideration of the operating speed and the external disturbance.

$$\begin{bmatrix}\dot{x}_1(t)\\ \dot{x}_2(t)\\ \dot{x}_3(t)\\ \dot{x}_4(t)\\ \dot{x}_5(t)\end{bmatrix} = \begin{bmatrix}0 & 100 & 0 & 0 & 0\\ -10^4 & -10^3 & 0 & 0 & 0\\ 0 & -10 & 0 & 10 & 0\\ 0 & 10 & -10 & -10 & 0\\ 0 & 0 & 0 & 100 & -10\end{bmatrix}\begin{bmatrix}x_1(t)\\ x_2(t)\\ x_3(t)\\ x_4(t)\\ x_5(t)\end{bmatrix} + \begin{bmatrix}0 & 0\\ 10^4 & 0\\ 0 & 0\\ 0 & 10\\ 10 & 0\end{bmatrix}\begin{bmatrix}250\times\Delta c(t)\\ 0.25\times\Delta\ddot{q}_m(t)\end{bmatrix}, \tag{4}$$

$$\begin{bmatrix}y_1 = \Delta\hat{c}(t)\\ y_2 = \Delta\hat{\dot{c}}(t)\\ y_3 = \Delta\hat{\ddot{q}}_m(t)\\ y_4 = \Delta\hat{\dot{q}}_m(t)\\ y_5 = \Delta\hat{q}_m(t)\end{bmatrix} = \begin{bmatrix}1 & 0 & 0 & 0 & 0\\ 0 & 1 & 0 & 0 & 0\\ 0 & 1 & -1 & -1 & 0\\ 0 & 0 & 0 & 1 & 0\\ 0 & 0 & 0 & 0 & 1\end{bmatrix}\begin{bmatrix}x_1(t)\\ x_2(t)\\ x_3(t)\\ x_4(t)\\ x_5(t)\end{bmatrix} + \begin{bmatrix}0 & 0\\ 0 & 0\\ 0 & 1\\ 0 & 0\\ 0 & 0\end{bmatrix}\begin{bmatrix}250\times\Delta c(t)\\ 0.25\times\Delta\ddot{q}_m(t)\end{bmatrix}. \tag{5}$$

The data for the electromagnets and levitation controller are described in Table 2.

2.3. *Guideway*

As reducing the weight is one of the primary issues in a Maglev guideway system, an in-depth design is required to avoid resonance by the structural vibration of levitation system, bogie

Table 2. Data for the levitation control system.

Item	Specification	Item	Specification
μ_0	$4\pi \times 10^{-7}$	k_1	7
N (Turn)	400	k_2	40
A (m^2)	0.036	k_3	4
R (Ω)	0.6	k_4	40
c_0 (m)	0.008	k_5	7
i_0 (A)	24		

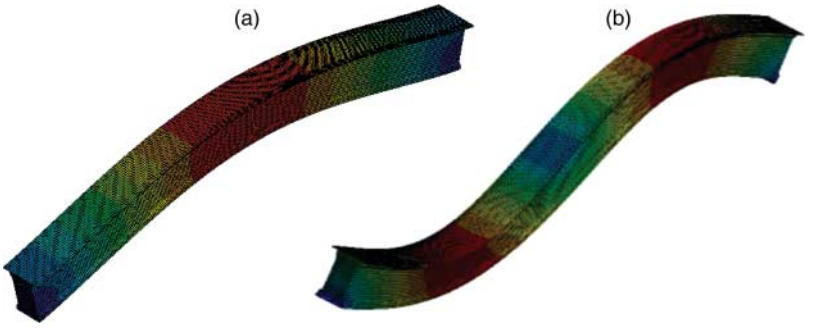

Figure 4. Vibration mode of guideway. (a) First vertical bending mode, 7.2 Hz and (b) second vertical bending mode, 25 Hz.

and car body. The elevated guideway is represented as a two-dimensional flexible beam by using modal superposition, which is the traditional modelling method. This is because the vibration by bending is relatively dominant compared the twist in a low speed Maglev system. In addition to, it could be said that there is choice to reduce calculation time. But the 3D model for guideway must consider the twist mode in the event of a short radius curve. The vibration mode analysis is conducted, and the results are shown in Figure 4. The first and second bending modes are only considered for the guideway model, because they are dominant compared to the twist mode. Meanwhile, acceleration spectrums of the guideway obtained from modal tests are shown in Figure 5. The natural frequency and damping ratio of guideway are 7.2 Hz and 1.1%, respectively, for first bending mode and 25 Hz and 2.4%, respectively, for second bending mode. Therefore, we can see that the vibration characteristics of the guideway model agree well with the results of the modal test as shown in Figure 5. The natural frequency of girder, which is located in the low frequency range, causes significant dynamic interactions between vehicle and guideway, and these influence the levitation stability of the Maglev system. The parameters of guideway are shown in Table 3.

According to the theory of the mode superposition, the deflection of the guideway can be expressed as the product of the shape and the generated coordinate, as follows:

$$u(x,t) = \sum_{n=1}^{N} q_n(t)\phi_n(x), \tag{6}$$

$$M_n\ddot{q}_n + C_n\dot{q}_n + K_n q_n = \phi_n^{\mathrm{T}} P(x,t), \tag{7}$$

where, $q_n(t)$ is general coordinate, $\phi_n(x)$ is mode shape function, and $P(x,t) = \sum_{i=1}^{N\mathrm{car}} \sum_{j=1}^{N\mathrm{bogie}} \sum_{k=1}^{N\mathrm{ems}} \sum_{l=1}^{N\mathrm{discretForce}} F_m(x,t)$, and $F_m(x,t)$ is electromagnet force in Equation (1). Modal properties such as modal mass, damping and stiffness which are obtained from the FE model and modal test are applied to the dynamic equation of the guideway, which is a set

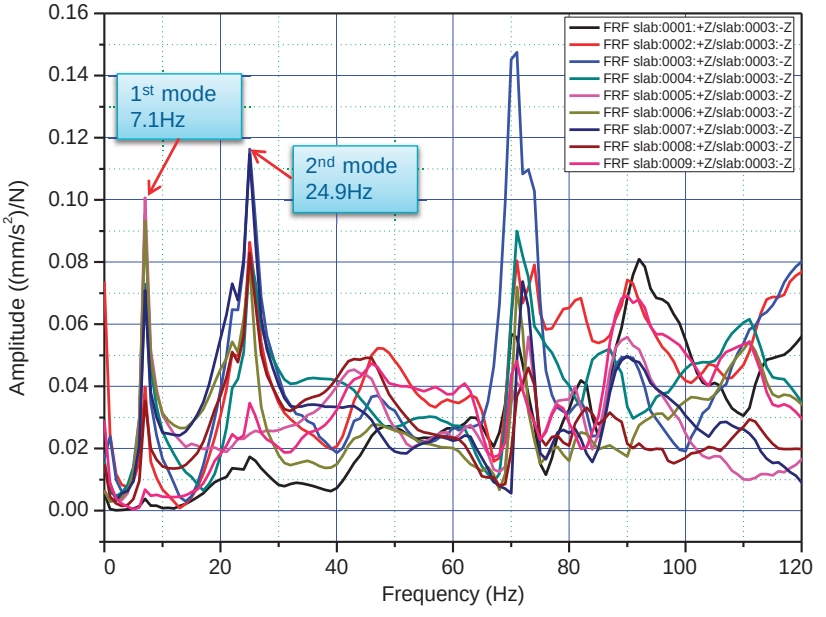

Figure 5. Measured acceleration spectrum of guideway.

Table 3. Properties for guideway.

Item		Specification	Item		Specification
Section area		1.24 m^2	Length		25 m
Density		22,000 kg/m^3	I		0.64673 m^4
Inertia		1.037 m^4	Young' modulus		28,825 Mpa
Natural	First	7.1 Hz	Damping ratio	First	1.08%
frequency	Second	24.9 Hz	ratio	Second	2.41%

of ordinary differential equations. The motion equation of the guideway is expressed in the form of Equation (8) and transformed to the state-space equation to combine the equations of vehicle and controller. The resulting state-space function is expressed as Equation (8).

$$\begin{aligned} \dot{x}(t) &= Ax(t) + \mathrm{BP}(x,t), \\ y(x,t) &= Cx(t) + \mathrm{DP}(x,t), \end{aligned} \tag{8}$$

where,

$$x = [q(t), \dot{q}(t)]^{\mathrm{T}}, \quad y = [u, \dot{u}, \ddot{u}]^{\mathrm{T}},$$

$$A = \begin{pmatrix} 0 & I \\ -M^{-1}K & -M^{-1}C \end{pmatrix}, \quad B = \begin{pmatrix} 0 \\ M^{-1}\phi^{\mathrm{T}} \end{pmatrix}, C = \begin{pmatrix} \phi & 0 \\ 0 & \phi \\ -\phi M^{-1}K & -\phi M^{-1}C \end{pmatrix},$$

$$D = \begin{pmatrix} 0 \\ 0 \\ \phi M^{-1}\phi^{\mathrm{T}} \end{pmatrix}.$$

Meanwhile, the surface roughness of the guideway is considered as one of the main sources of vibration of the Maglev system. Therefore it needs to generate the random irregularity

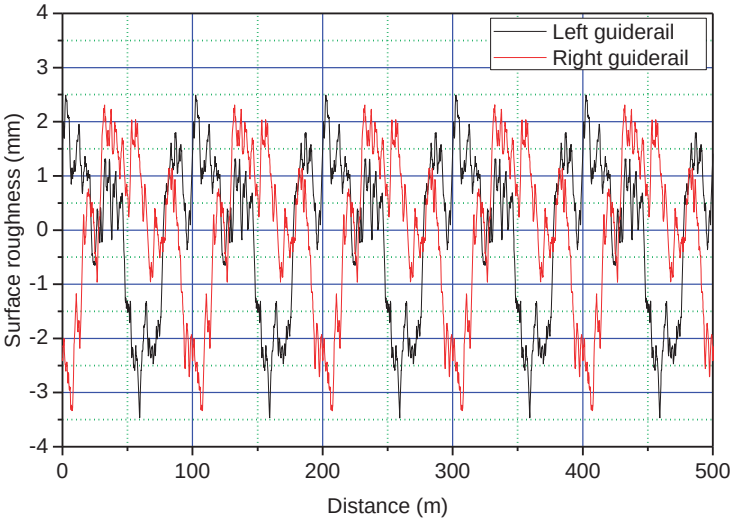

Figure 6. Surface roughness profile.

profile to predict dynamic behaviour in the time domain. The generated random irregularity profiles are shown in Figure 6.[17] In this paper, the irregularity profile and guideway deflection is combined, and they are directly used as composite disturbance inputs to Maglev vehicle dynamic simulation.

2.4. *Coupled model*

The equations of motion for the EMS, vehicle, and guideway are included in the integrated to be able to predict the dynamic response as shown in Figure 7. The equations of motion for the vehicle, a constrained mechanical system, are composed of the following Equations (9)–(12). The equations for the electromagnet and guideway are incorporated into the equations for the vehicle. The levitation forces are added to the right side of Equation (9).

$$\begin{bmatrix} \boldsymbol{M} & \boldsymbol{\Phi}_q^{\mathrm{T}} \\ \boldsymbol{\Phi}_q & \boldsymbol{0} \end{bmatrix} \begin{bmatrix} \ddot{\boldsymbol{q}} \\ \boldsymbol{\lambda} \end{bmatrix} = \begin{bmatrix} \boldsymbol{Q}^A + F_m \\ \gamma \end{bmatrix}, \tag{9}$$

$$\boldsymbol{\Phi}(\boldsymbol{q}, t) = [\Phi_1(\boldsymbol{q}, t), \ldots, \Phi_m(\boldsymbol{q}, t)]^T = \boldsymbol{0}, \tag{10}$$

$$\boldsymbol{\Phi}_q \dot{\boldsymbol{q}} = -\boldsymbol{\Phi}_t \equiv \boldsymbol{v}, \tag{11}$$

$$\boldsymbol{\Phi}_{\mathbf{q}} \ddot{\boldsymbol{q}} = -(\boldsymbol{\Phi}_{\mathbf{q}} \dot{\boldsymbol{q}})_{\mathbf{q}} \dot{\boldsymbol{q}} - 2\boldsymbol{\Phi}_{\mathbf{qt}} \dot{\boldsymbol{q}} - \boldsymbol{\Phi}_{tt} \equiv \boldsymbol{\gamma}, \tag{12}$$

where $\boldsymbol{q}(t)$ is the position, $\dot{\boldsymbol{q}}(t)$ the velocity, $\ddot{\boldsymbol{q}}(t)$ the acceleration, $\mathbf{M}(t)$ mass matrix, $\boldsymbol{\Phi}_{\boldsymbol{q}}(t) \equiv [\partial \boldsymbol{\Phi}_j / \partial \boldsymbol{q}_i]_{m \times n}$ the Constraint Jacobian, $\boldsymbol{Q}^{\boldsymbol{A}}(t)$ the external force and $\boldsymbol{\lambda}(t)$ the Lagrange multiplier.

A procedure for dynamic simulation is shown in Figure 8. This paper uses LMS Virtual.Lab Motion as a dynamic analysis tool for generating and solving equations of motion. Equations of levitation control and guideway system are defined in the user-defined subroutine of LMS Virtual.Lab Motion. The user-defined subroutine detects the air gap and its derivative. Then, the subroutine evaluates the system of differential equations of the Maglev system, and calculates the levitation forces. The forces are applied to both the electromagnet and guideway in the subroutine.

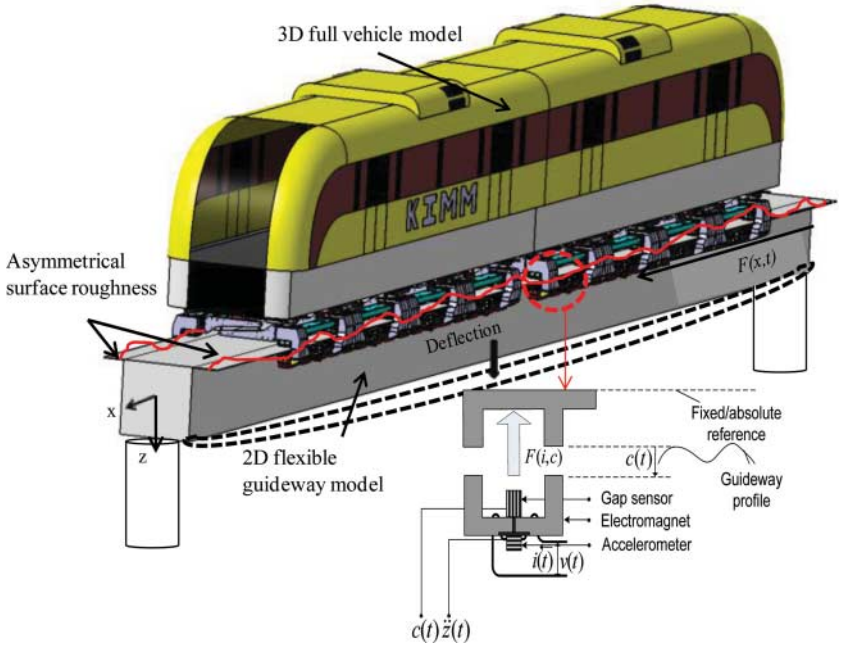

Figure 7. An integrated elaborated analysis model.

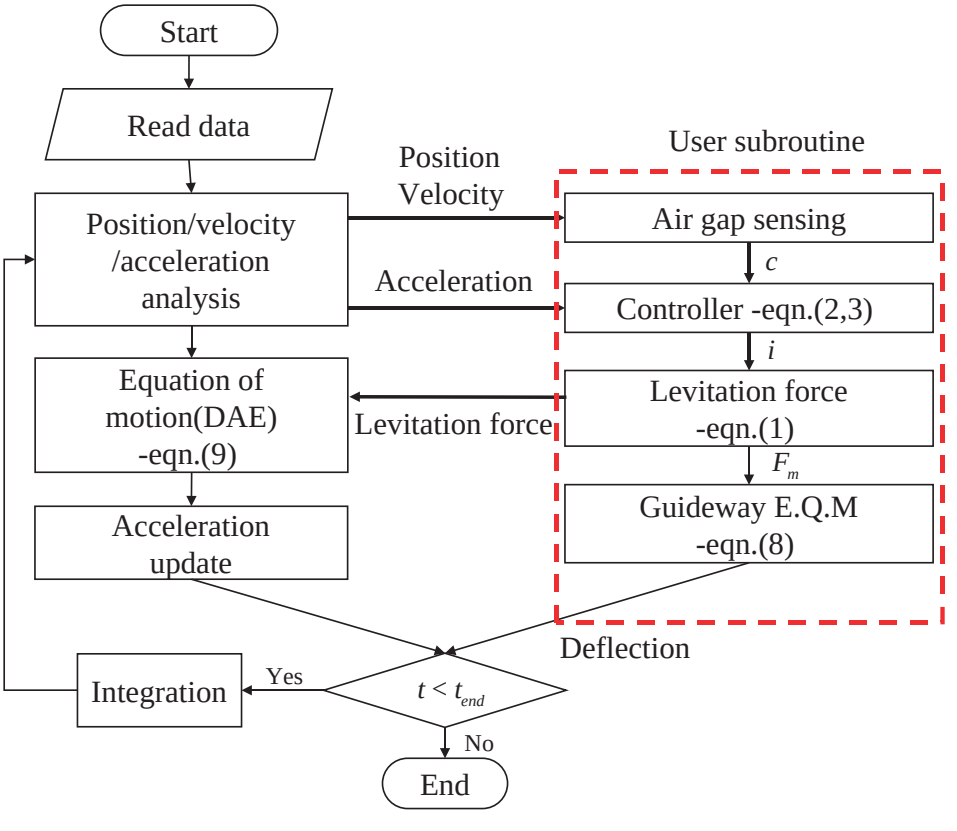

Figure 8. Procedure of dynamic simulation.

3. Simulation

3.1. *Excitation*

There are various sources that produce vibrations in an EMS-type Maglev that runs over an elevated guideway. To represent such exciting vibration forces, the force having amplitude and frequency of Equation (13) is applied to the mid-span of the guideway which has largest deflection as shown in Figure 9. This sine function is adopted to excite the guideway with the frequencies which have the range of operating the levitation controller, 0–100 Hz and to investigate frequency response characteristics of Maglev vehicles. The height of amplitude is set with a value that can clearly show the frequency response of the system.

$$F_v(t) = A \sin(\pi t^2). \tag{13}$$

3.2. *Verification*

To demonstrate the feasibility of the proposed model, the mid-span deflections of the guideway and air gaps are measured to compare the results of the simulation with those of the test. Figures 10 and 11 show the measured air gaps and mid-span guideway deflections from test and simulation, respectively. As the maximum deflection is 3.7 mm for test and 3.5 mm for simulation, it can be said that there is not much difference between the two solutions. The RMS of air gaps obtained from test and simulation also show similarity, at 8.02 and 8.01 mm, respectively. It can be seen that the proposed model has reliability through the comparative study.

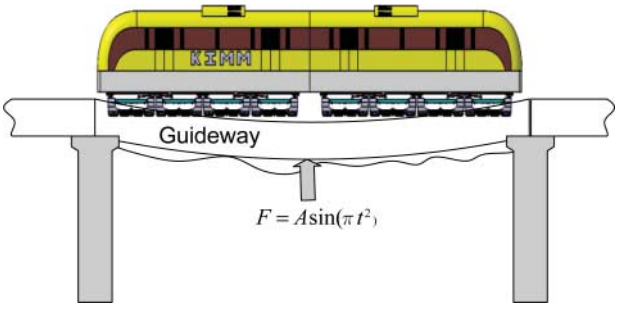

Figure 9. Excitation point.

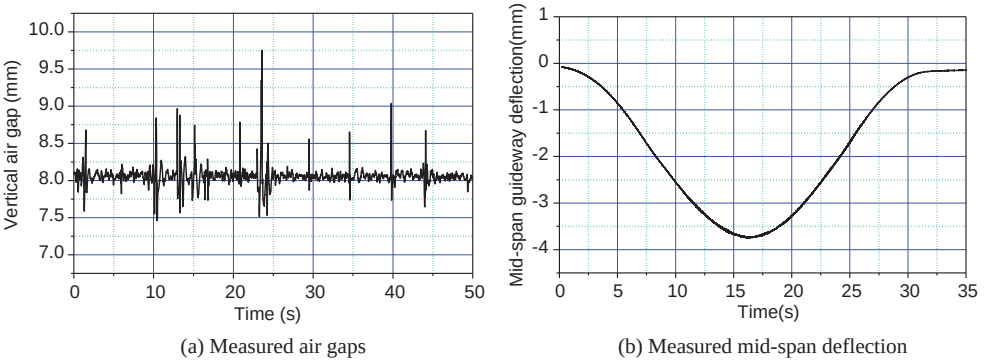

(a) Measured air gaps (b) Measured mid-span deflection

Figure 10. Measured air gaps and deflection when Maglev is moving at around 5 km/h.

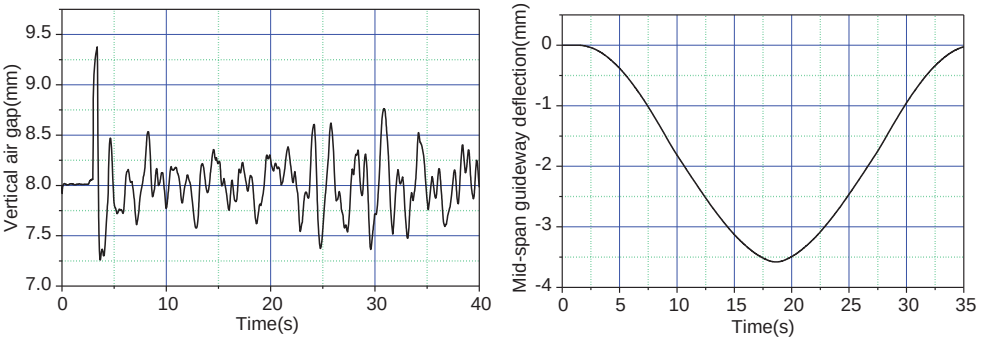

(a) Simulated air gaps (b) Simulated mid-span deflection

Figure 11. Simulated air gaps and deflection at 5 km/h.

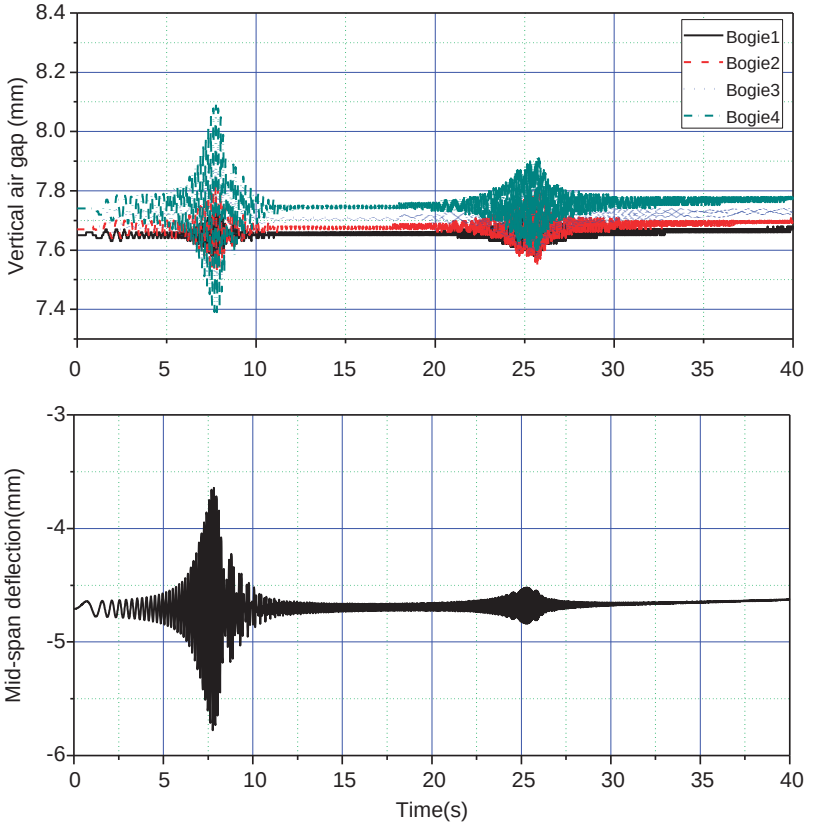

Figure 12. Air gaps and deflection at standstill.

3.3. *Standstill*

In an EMS-type Maglev vehicle, resonance occurs occasionally when the vehicle is levitated over the guideway, standing still at the speed of 0 km/h. That is to say, there is excitation as shown in Figure 11 when the vehicle is suspended over the guideway without moving. Figure 12 shows vertical air gaps and mid-span deflection of the guideway of each bogie. As shown in Figure 12, it can be seen that air gaps and mid-span deflection of the guideway at 7 s (7 Hz) and 25 s (25 Hz) are dominant. To investigate guideway frequency response

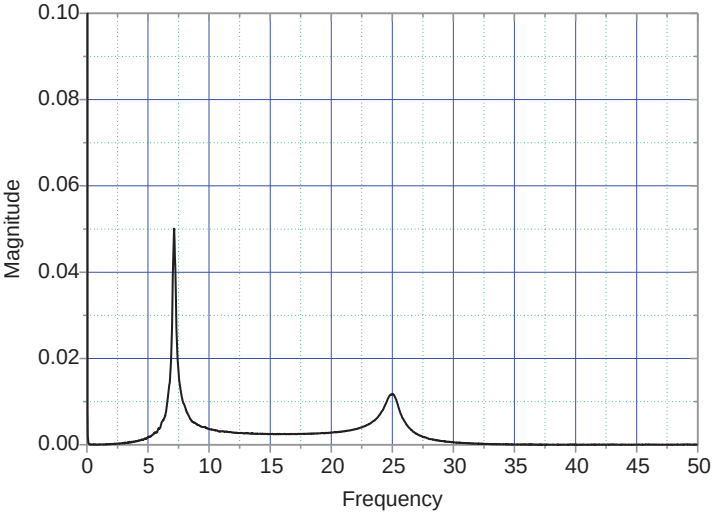

Figure 13. Frequency analysis of air gap deviation at standstill.

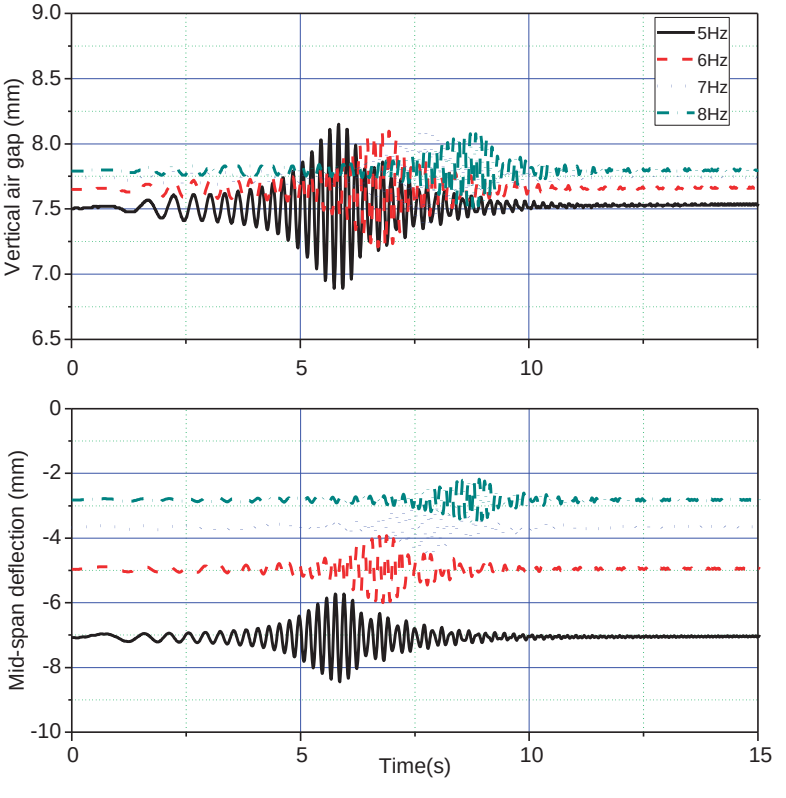

Figure 14. Air gaps and deflection of different guideways.

more clearly, frequency domain analysis of the air gaps is carried out, as can be seen in Figure 13. The two frequencies correspond to the first and second natural frequency of the guideway. Resonance may occur at these frequencies, and so sufficient damping to stabilise is required. This damping can be determined by the optimisation of gains such as Equation

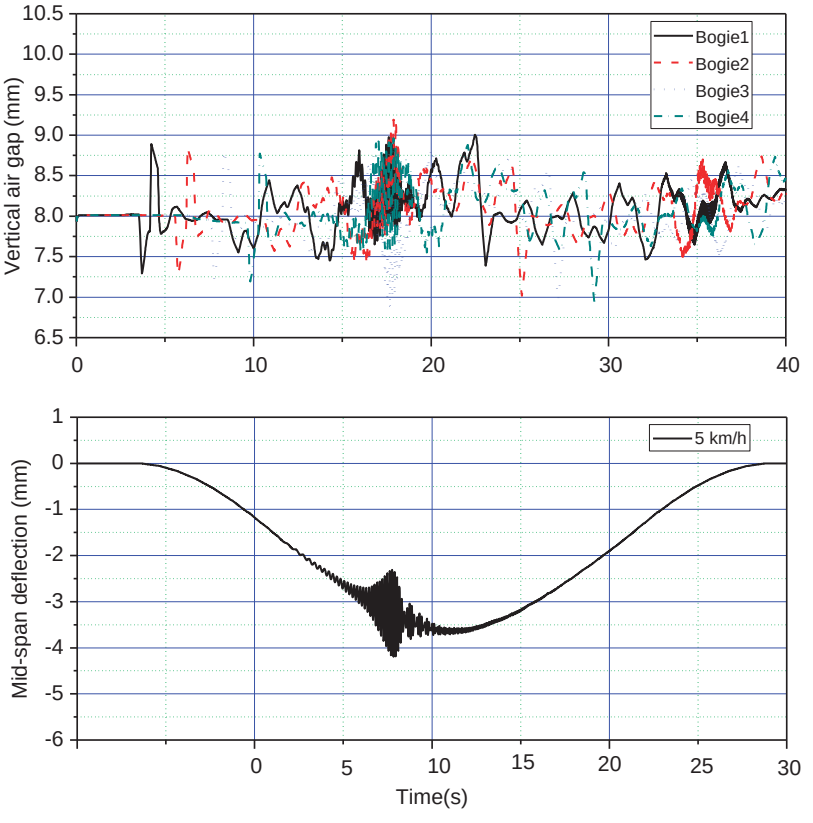

Figure 15. Air gaps and deflection during moving.

(3). Thus, it can be seen that the proposed model, which is a detailed and integrated dynamic model, is sufficiently feasible to evaluate stability throughout the system vibration analysis. Consequently, it can be said that the proposed model is helpful to design levitation system, vehicle suspension and structural characteristics of the guideway for ensuring stability.

Next, an analysis that assumes the change of the mass and stiffness is carried out to establish design direction for a slender guideway. Figure 14 shows air gaps and mid-span deflection when first natural frequency of the guideway varies to 5, 6, 7 and 8 Hz, respectively. The air gaps and mid-span deflection of guideway with first natural frequency of 5 Hz are the largest, and it can be seen that the air gaps and mid-span deflection are reduced as the natural frequency increase. Therefore, the guideway's vibration characteristics should be limited to consider the reduction of weight and levitation stability simultaneously. In the long run, the design direction for the slender guideway is desired to reduce construction cost, but limits should be set to retain the levitation stability.

3.4. *Low speed running*

Our experience showed that resonance occurred occasionally during running at low speeds of under 10 km/h. To investigate vibration response during running at low speed, dynamic analysis is carried out. The vertical surface irregularity of the guideway as shown in Figure 6 is considered, and the speed of the vehicle is 5 km/h. Figures 15 and 16 show air gaps and mid-span deflection in the time and frequency domains. It can be seen that the amplitude of vibration is the largest at near maximum deflection. The results from frequency analysis

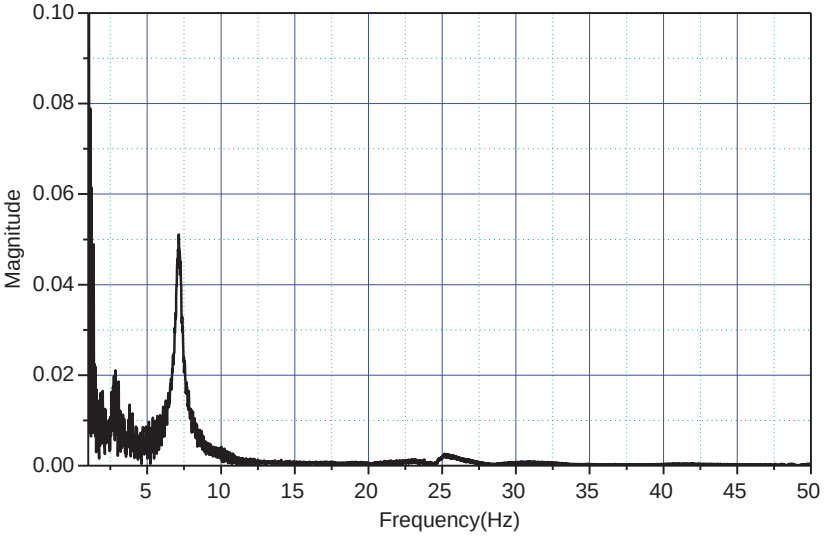

Figure 16. Frequency analysis of air gaps on the coupled resonance during moving.

show that the magnitude of vibration increases at first and second natural frequency of the guideway. Thus, it can be concluded that the guideway's structural characteristics and stable control algorithm are essential to suppress the resonance, because it may mostly occur during running at low speeds.

4. Conclusion

To investigate the levitation stability of an EMS-type Maglev vehicle, a more detailed model is proposed. The proposed model is an integrated 3D full vehicle model based on virtual prototyping, 2D flexible guideway by using the modal superposition, feedback controller and guideway irregularities into a whole system. The model, which considers the dynamic characteristics of all subsystems in detail, has advantages in terms of evaluating the stability of the levitation system. The feasibility of the integrated model is verified as it represents the similarities to the dynamic behaviour of an actual vehicle. By applying the proposed model to a Maglev vehicle, the vibration characteristics of the system are investigated, and it is confirmed that the controller used in an actual Maglev vehicle has stability. In the future, an expansion of the 3D guideway model to consider the effects of lateral and twisting characteristics is recommended.

Disclosure statement

No potential conflict of interest was reported by the authors.

Funding

This research was supported by a grant [14 RTRP-B070539-02] from Railroad Technology Research Program funded by Ministry of Land, Infrastructure and Transport of Korean government.

References

[1] Zhou D, Hansen CH, Li J, Chang W. Review of coupled vibration problems in EMS Maglev vehicle. Int J Acoust Vib. 2010;15(1):10–23.

[2] Yabuno H, Kanda R, Lacarbonara, W, Aoahima N. Nonlinear active cancellation of the parametric resonance in a magnetically levitated body. J Dyn Syst Meas Control. 2004;126(3):433–442.
[3] Han HS, Yim BH, Lee NJ, Hur YC, Kim SS. Effect of guideway's vibrational characteristics on dynamics of a Maglev vehicle. Veh Syst Dyn. 2009;47(3):309–324.
[4] Cai Y, Chen SS, Rote DM, Coffey HT. Vehicle/guideway interaction for high speed vehicles on a flexible guideway. J Sound Vib. 1994;175(5):625–646.
[5] Zhao CF. Maglev vehicle system dynamics [Ph.D. dissertation]. Southwest Jiaotong University; 2002.
[6] Hâgele N, Dignath F. Vertical dynamics of the maglev vehicle transrapid. Multibody Syst Dyn. 2009;21: 213–231.
[7] Zhao CF, Zhai WM. Maglev vehicle/guideway vertical random response and ride quality. Veh Syst Dyn. 2002;38(3):116–132.
[8] Shu GW, Meisinger R, Shen G. Modeling and simulation of Shanghai MAGLEV train transrapid with random track irregularities. Sonderdruck Schriftenreihe der Georg-Simon-Ohm-Fachhoch-schule Nürnberg Nr. 39; July 2007.
[9] Shu GW, Meisinger R, Shen G. Simulation of a MAGLEV train with periodic guideway deflections. Asia Simulation Conference – 7th International Conference on System Simulation and Scientific Computing; 2008. p. 421–425.
[10] Dai HG. Dynamic behavior of maglev vehicle/guideway system with control [Ph.D. dissertation]. Case Western Reserve University; 2005.
[11] Zheng XJ, Wu JJ, Zhou YH. Numerical analysis on dynamic control of five-degree-of-freedom maglev vehicle moving on flexible guideways. J Sound Vib. 2000;235(1):43–61.
[12] Zhao CF, Zhai WM, Wang KY. Dynamic responses of the low-speed Maglev vehicle on the curved guideway. Veh Syst Dyn. 2002;38(3):185–210.
[13] Yim BH, Han HS, Lee JK, Kim SS. Curving performance simulation of an EMS-type Maglev vehicle. Veh Syst Dyn. 2009;47(10):1287–1304.
[14] Yau JD. Vibration control of maglev vehicles traveling over a flexible guideway. J Sound Vib. 2009;321: 184–200.
[15] Han HS, Kim YJ, Shin BC, Kim BH. Simulation of dynamic interaction between maglev and guideway using FEM. Maglev 2006, Dresden; 2006.
[16] Shi XH, She LH, Chang WS. Vibration analysis of elastic-rigid coupling EMS maglev system. Maglev 2004, Shanghai; 2004.
[17] Han HS, Yim BH, Lee NJ, Kim YJ. Prediction of ride quality of a Maglev vehicle using a full vehicle multi-body dynamic model. Veh Syst Dyn. 2009;47(10):1271–1286.
[18] Sinha PK. Electromagnetic suspension-dynamic and control. London: IEE; 1987.